Tumor Biol. (2014) 35:11027–11039
DOI 10.1007/s13277-014-2396-9

RESEARCH ARTICLE

Mitochondrial and caspase pathways are involved in the induction of apoptosis by IB-MECA in ovarian cancer cell lines

Hamideh Abedi · Mahmoud Aghaei · Mojtaba Panjehpour · Sima Hajiahmadi

Received: 17 May 2014 / Accepted: 23 July 2014 / Published online: 6 August 2014

Abstract A_3 adenosine receptor agonist (IB-MECA) has been shown to play important roles in cell proliferation and apoptosis in a variety of cancer cell lines. The present study was designed to understand the mechanism underlying IB-MECA-induced apoptosis in human ovarian cancer cell lines. The messenger RNA (mRNA) and protein expression levels of A_3 adenosine receptor were detected in OVCAR-3 and Caov-4 ovarian cancer cells. IB-MECA was capable of decreasing intracellular cyclic adenosine monophosphate (cAMP) that was the reason for the presence of functional A_3 adenosine receptor on the cell lines. IB-MECA significantly reduced cell viability in a dose-dependent manner. Cytotoxicity of IB-MECA was suppressed by MRS1220, an A_3 adenosine receptor antagonist. The growth inhibition effect of IB-MECA was related to the induction of cell apoptosis, which was manifested by annexin V-FITC staining, activation of caspase-3 and caspase-9, and loss of mitochondrial membrane potentials ($\Delta\Psi m$). In addition, downregulation of the regulatory protein Bcl-2 and upregulation of Bax protein by IB-MECA were also observed. These findings demonstrated that IB-MECA induces apoptosis via the mitochondrial signaling pathway. These suggest that A_3 adenosine receptor agonists may be a potential agent for induction of apoptosis in human ovarian cancer cells.

Keywords Ovarian cancer · IB-MECA · Apoptosis · A_3 adenosine receptor · Caspase

H. Abedi · M. Aghaei (✉) · M. Panjehpour · S. Hajiahmadi
Department of Clinical Biochemistry, School of Pharmacy and Pharmaceutical Sciences, Isfahan University of Medical Sciences, P.O. Box: 81746-73461, Isfahan, Iran
e-mail: maghaei@pharm.mui.ac.ir

M. Panjehpour
Bioinformatics Research Center, Isfahan University of Medical Sciences, Isfahan, Iran

Introduction

Human ovarian cancer is the fourth most common cancer and the fifth leading cause of cancer-related deaths among women [1–3]. The standard treatment for this disease is surgery and chemotherapy [1]. One of the main strategies in the treatment of cancer is identification of drugs that can cause apoptotic death in malignant cells [4, 5]. In this context, adenosine 5′-triphosphate (ATP), UTP, and adenosine are considered to be the agents that inhibit the growth of several cancerous cell lines [6, 7].

The purine nucleoside adenosine is a regulatory metabolite that is the product of ATP catabolism and is released from cells under injury, stress, and hypoxia [8]. Adenosine has several physiological and pharmacological functions such as modulating proliferation, inhibiting cell growth, and inducing apoptosis in various cancer cell types [9]. The effects of adenosine are related to its interaction with adenosine receptors which are classified into four subtypes: A_1, A_2A, A_2B, and A_3 [10].

These cell surface adenosine receptors are members of the superfamily of G-protein-coupled receptors (GPCRs). The A_2A and A_2B receptors linked to GS proteins activate adenylate cyclase, and their stimulation increases cAMP. The A_1 and A_3 receptors interact with Gi proteins, inhibit adenylate cyclase, and lead to a reduction of intracellular cyclic adenosine monophosphate (cAMP) concentration [11].

Adenosine receptors play an important role in cell growth and proliferation in different cell lines [12]. The A_3 adenosine receptor (A_3AR) expression level in normal cells is low, while it is more highly expressed in various tumor cells [13]. The role of A_3AR in protecting cells against death and also inducing apoptosis is dependent on agonist concentration, cell type, rate of receptor activation, and signaling mechanisms [14, 15]. The A_3AR agonist can induce apoptosis [16], necrosis [17], or cell cycle arrest in cancer cell lines [14].

It was shown that IB-MECA, an A_3AR agonist, inhibits the growth of different cancer cell types like melanoma, colon, breast, leukemia, and prostate [18–22]. It has been demonstrated that A_3AR is expressed in both estrogen receptor-positive and receptor-negative breast cancer cell lines and IB-MECA-inhibited cell growth [23]. This inhibition was reversed by using the selective A_3AR antagonist, indicating the specificity of the response [24]. Recently, it was reported that IB-MECA suppressed cell proliferation via cell cycle arrest and induced apoptosis in human prostate cancer cell lines. Also increase in sub-G1 population, activation of caspase-3, and downregulation of Bcl-2 expression were observed [22]. Moreover, induction of apoptosis caused by A_3AR agonist was demonstrated in hepatocellular carcinoma by an increase in the pro-apoptotic proteins Bad, Bax expression levels, and caspase-3 [25].

In a recent study, the effect of adenosine on OVCAR-3 ovarian cancer cells has been investigated. It was reported that adenosine can induce apoptosis and cell cycle arrest via the extracellular pathway [7], but the mechanism effects of adenosine and A_3 adenosine receptor agonists in human ovarian cancer cell lines have not been illustrated. With respect to these issues, the aims of this study were twofold: first, whether A_3AR is validated in the ovarian cancer cell lines by looking at the correlation between receptor expression and its function; and second, whether A_3AR agonist and antagonist modulate cell growth or induce apoptosis in human ovarian cancer cells. The molecular mechanisms underlying apoptosis were also studied.

Materials and methods

Chemical reagents

Culture media (RPMI 1640) and growth supplements (trypsin/EDTA, phosphate-buffered saline (PBS), penicillin and streptomycin, fetal bovine serum (FBS)) were provided by Gibco (Rockville, USA). Caspase-3 and caspase-9 colorimetric assay kits were purchased from R&D Systems Co. (Minneapolis, USA). Annexin V-FITC apoptosis detection kit was obtained from BioVision (USA). 3-(4,5-Dimethyl thiazol-2-yl)-2,5 diphenyltetrazolium bromide (MTT); dimethyl sulfoxide (DMSO); 5,5′,6,6′-tetrachloro-1,1′,3,3′-tetraethylbenzimidazolylcarbocyanine iodide (JC-1); 1-deoxy-1-[6-[[(3-iodophenyl)methyl]amino]-9H-purine-9-yl]-*N*-methyl-b-D-ribofuranuronamide (IB-MECA), an A_3 receptor agonist; 9-chloro-2-(2-furanyl)-5-(phenylacetyl)amino][1,2,4,]-triazolo[1,5-c] quinazoline (MRS1220), an adenosine A_3 receptor antagonist; forskolin (adenylate cyclase activator); Ro-20-1724 (phosphodiesterase inhibitor); cAMP direct immunoassay (ELISA) kit; and Z-VAD-fmk were purchased from Sigma-Aldrich (St. Louis, MO, USA). RevertAid M-MuLV Reverse Transcriptase was obtained from Fermentas (Ontario, Canada). Rabbit polyclonal A_3 adenosine receptor antibody and anti-rabbit IgG-HRP antibody were purchased from Acris (Germany). Mouse monoclonal anti-Bcl-2, anti-Bax antibodies, and horseradish peroxidase (HRP)-conjugated anti-mouse IgG were purchased from Santa Cruz Biotechnology (Santa Cruz, CA, USA).

Cell culture

Human ovarian cancer cell lines OVCAR-3 and Caov-4 were obtained from the National Cell Bank of Iran (NCBI). Cell lines were grown in RPMI 1460 supplement with 10 % FBS, 100 U/ml of penicillin, and 100 μg/ml of streptomycin. They were incubated at 37 °C in a humidified incubator with 5 % CO_2 and 95 % air.

Gene expression assay

For expression profile analysis, total RNA was extracted by TRIzol reagent (Sigma-Aldrich). RNA concentration and purity were carried out by a UV spectrophotometer. Then, total RNA was reverse-transcribed using RevertAid First Strand cDNA synthesis kit with random hexamer according to the manufacturer's protocol (Fermentas Cat. No. K1631).

Quantitative real-time RT-PCR assays of A_3 adenosine receptor cDNA were carried out using gene-specific double fluorescently labeled TaqMan MGB probe (HS00252933-mL) in a fast real-time PCR system (ABI 7500 fast Real-Time PCR System, Applied Biosystems, Foster City, USA) in accordance with the manufacturer's recommendations. For the real-time RT-PCR of the genes, TaqMan probe GAPDH (HS99999905-m1) was used as an internal control in order to normalize following the manufacturer's recommendations. The relative messenger RNA (mRNA) expression level was determined using the $2^{-\Delta\Delta Ct}$ analysis method.

Western blot analysis

The cells were seeded 24 h prior to assay into six-well plates (5×10^5 cells/ml) and were grown as a confluent monolayer. The A_3 adenosine receptor, Bcl-2, and Bax protein content were detected by western blot analysis. At first, the cells were treated with different concentrations (1–100 μM) of IB-MECA and incubated for 48 h. For A_3 adenosine receptor protein content assay, the cells were not treated with IB-MECA. Then, cells were lysed in RIPA buffer (150 mmol/l NaCl, 50 mmol/l Tris-HCl, pH 8, 0.5 % sodium deoxycholate, 1 % Nonidet P-40, 1 mmol/l phenylsulfonylfluoride, 10 μg/ml aprotinin, 100 μmol/l sodium orthovanadate) for 2 h at 4 °C. After centrifugation at 10,000*g* for 10 min, the supernatant was removed and the sediment was discarded. Equal amounts of proteins were applied to SDS-polyacrylamide gel for

electrophoresis and then transferred onto a PVDF membrane. The membrane was blocked with skim milk for 2 h and then incubated with primary antibodies for 2 h at room temperature. Then, the membrane was washed with PBS-T three times. After incubating with the required secondary antibody and rewashing three times, the signals were visualized by enhanced chemiluminescence (Amersham).

Cyclic AMP measurement

The cells were seeded 24 h prior to assay into 24-well plates (3×10^5 cells/ml) and were grown as a confluent monolayer. The cells were then washed twice with Hank's HEPES buffer solution (HHBS) (20 mM, pH 7.4). After 15 min, the medium was replaced with fresh HHBS containing ADA 2 U/ml and Ro-20-1724 (100 μM) (as phosphodiesterase inhibitor) and incubated for 15 min at 37 °C after which different concentrations (0.01–100) of IB-MECA in the presence and absence of A_3AR antagonist, MRS1220 (1 μM), plus 10 μM forskolin (as stimulator of adenylyl cyclase) were added to the mixture and incubated for 10 min. At the end of incubation, the solution was aspirated and replaced immediately with ice-cold HCl 0.1 M. The level of cAMP accumulation was determined using EIA kit (acetylated version). Dose-response curves were calculated using GraphPad Prism.

MTT viability assay

Cell viability was determined by the MTT assay as described previously [26]. Briefly, approximately 5,000 cells/well were seeded in 96-well plates and incubated for 24 h. After cells were grown to 60–80 % confluency, the medium was replaced by fresh medium containing various concentrations (0.0001–100 μM) of IB-MECA in the presence and absence of MRS1220 (1 μM) and incubated for 48 h. At the end of the experiments, 20 μl of MTT (0.5 mg/ml in PBS) was added to each well and incubated at 37 °C for 4 h, then the medium culture was removed carefully, and the dye was dissolved with 200 μl of DMSO. The plates were incubated in the dark for an additional 10 min and absorbance was measured at a wavelength of 570 nm by a microplate reader (Tecan Sunrise Instruments, Austria). All assays were performed in triplicate.

Flow cytometry assay using annexin V/propidium iodide staining

To determine apoptosis of ovarian cancer cell lines, we employed annexin V-FITC/propidium iodide (PI) apoptosis detection kit and it was performed according to the manufacturer's protocol as described previously [26]. Briefly, OVCAR-3 and Caov-4 cells at a density of 5×10^5 cell/well in six-well plates were incubated for 24 h. Then, IB-MECA in the presence and absence of A_3AR antagonist, MRS1220 (1 μM) treatment, was carried out and the plates were once more incubated for 48 h. The treated and untreated cells were harvested and washed twice with cold PBS. The cell pellets were resuspended in 500 μl of 1× binding buffer, and 5 μl of annexin V-FITC and 5 μl of PI were added into the cell suspension, followed by gentle vortexing. The stained samples were incubated for 15 min at room temperature in a dark condition. The cells were analyzed by a Becton Dickinson flow cytometer (USA) using the software supplied in the instrument. This allows the discrimination of living cells (unstained with either fluorochrome) from early apoptotic cells (stained only with annexin V) and late apoptotic cells (stained with both annexin V and PI).

Measurement of caspase activity

Cells (3×10^5 per well) were cultured overnight in 24-well plates and treated with various concentrations (0.01–100 μM) of IB-MECA for an additional 6–48 h. Caspase-3 and caspase-9 activity was assessed according to the manufacturer's instruction of caspase colorimetric assay kit (R&D Systems). Briefly, cells were harvested and lysed in 50 μl lysis buffer on ice for 10 min and then centrifuged at 10,000*g* for 1 min. After centrifugation, the supernatants were incubated with caspase-3 and caspase-9 substrate in reaction buffer. Samples were incubated in 96-well flat bottom microplate at 37 °C for 1 h. The amount of released *p*-nitroaniline was measured using a microplate reader (Bio-Rad, Hercules, CA, USA) at 405 nm wavelength.

Mitochondrial membrane potential (ΔΨm) analysis

The mitochondrial membrane potential (ΔΨm) was estimated using a lipophilic cationic JC-1 probe as previously described by Ghavami et al. [27]. JC-1 is capable of selectively entering the mitochondria, where it forms monomers and emits green fluorescence when ΔΨm is relatively low. At a high ΔΨm, JC-1 aggregates and gives red fluorescence [28]. The ratio between green and red fluorescence provides an estimate of ΔΨm that is independent of the mitochondrial mass. OVCAR-3 and Caov-4 cells were plated in black clear-bottom 96-well plates. After treatment with IB-MECA (0.1–100 μM) in the presence and absence of A_3AR antagonist, MRS1220 (1 μM), for 6–48 h, cells were loaded with JC-1 by replacing the culture medium with HEPES buffer (40 mM, pH 7.4) containing 4.5 g/l glucose (high-glucose medium) or 1.5 g/l glucose (low-glucose medium), 0.65 % NaCl, and 2.5 μM JC-1 for 30 min at 37 °C, and then washed once with HEPES buffer. Fluorescence was measured using a Synergy HT Multi-Mode Microplate Reader (BioTek Instruments) that allows for the sequential measurement of each well at two excitation/emission wavelength pairs, 490/540 and 540/590 nm. Changes in the ratio between the measured red

(590 nm) and green (540 nm) fluorescence intensities indicate changes in mitochondrial membrane potential.

Statistical analysis

The results were expressed as mean±SD, and statistical analysis was performed by nonparametric analysis of variance between groups (ANOVA) followed by Dunnett's post hoc test. All experiments were repeated at least three times. Statistical analyses were done using the software package SPSS version 17. A difference was considered statistically significant at $P<0.05$.

Results

A_3AR mRNA and protein expression profiles in ovarian cancer cells

Differential expression of A_3 adenosine receptor in both cell lines was investigated by qRT-PCR using a TaqMan probe. A_3 adenosine receptor mRNAs were detected in the OVCAR-3 and Caov-4 cell lines, but in different levels. Results demonstrated that the expression level of mRNA in Caov-4 cell line was higher (1.8-fold) than that in OVCAR-3 cells (Fig. 1a).

To verify the mRNA expression findings of A_3 adenosine receptor, western blotting was performed on ovarian cancer cells. A single band (38 kDa) was detected in the western blot using the anti-A_3 receptor antibody in both cell lines (Fig. 1b). The protein band that was acquired from OVCAR-3 was weaker than that seen from Caov-4 (Fig. 1b). The band intensity of A_3 adenosine receptor was quantified by ImageJ software. Data analysis showed that A_3 protein expression in Caov-4 cells was higher (1.5-fold) than that in OVCAR-3 cell line (Fig. 1c).

Effect of A_3 adenosine receptor agonists on cyclic AMP accumulation

To evaluate the existence of functional A_3 receptors in OVCAR-3 and Caov-4 cells and to evaluate whether changes of mRNA and protein expression were reflected at a functional level, we determined the potency of the IB-MECA in the inhibition of cAMP levels. IB-MECA was able to inhibit forskolin-stimulated cAMP levels with an EC_{50} value of 0.82 μM in OVCAR-3 cells ($P<0.05$) (Fig. 2a). As it is shown in Fig. 2b, IB-MECA was able to inhibit forskolin-stimulated cAMP levels with an EC_{50} value of 1.2 μM in Caov-4 cells ($P<0.01$). The A_3 adenosine receptor antagonist, MRS1220, antagonized IB-MECA-induced inhibitions of cAMP levels in both cell lines, suggesting the involvement of A_3 receptors (Fig. 2a, b).

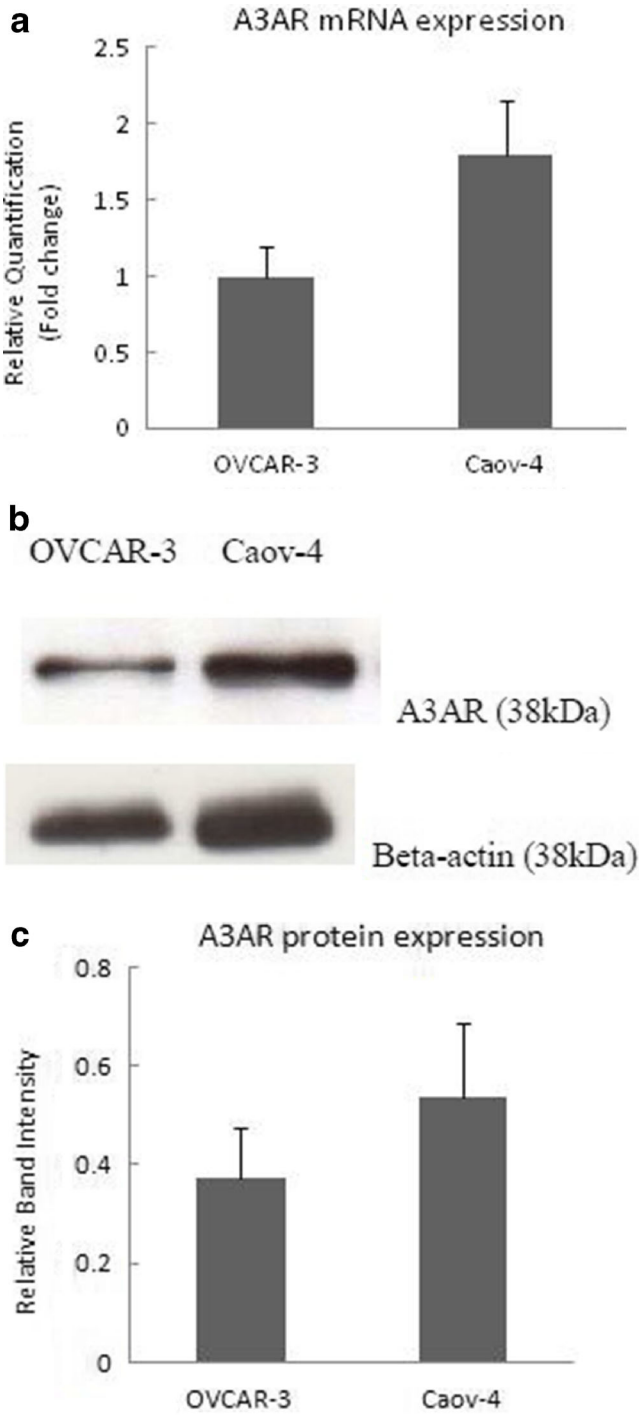

Fig. 1 Real-time PCR and western blot analysis of A_3 adenosine receptor expression in the human ovarian cancer cell lines OVCAR-3 and Caov-4. The relative expression level of A_3 adenosine receptor in OVAR-3 cell line was higher than that in Caov-4 cell line (**a**). The data are representative of three independent experiments, and the relative expression values were calculated using the equation $RQ=2^{-\Delta\Delta Ct}$. Western blotting detection of A_3 adenosine receptor protein expression in ovarian cancer cell lines (**b**). A 38-kDa band was detected in the western blot using the anti-A_3 receptor. The relative expression level of A_3 adenosine receptors in OVCAR-3 cell line was higher than that in Caov-4 cell line (**c**). The data are representative of three independent experiments, and the relative expression values were calculated using the ImageJ software

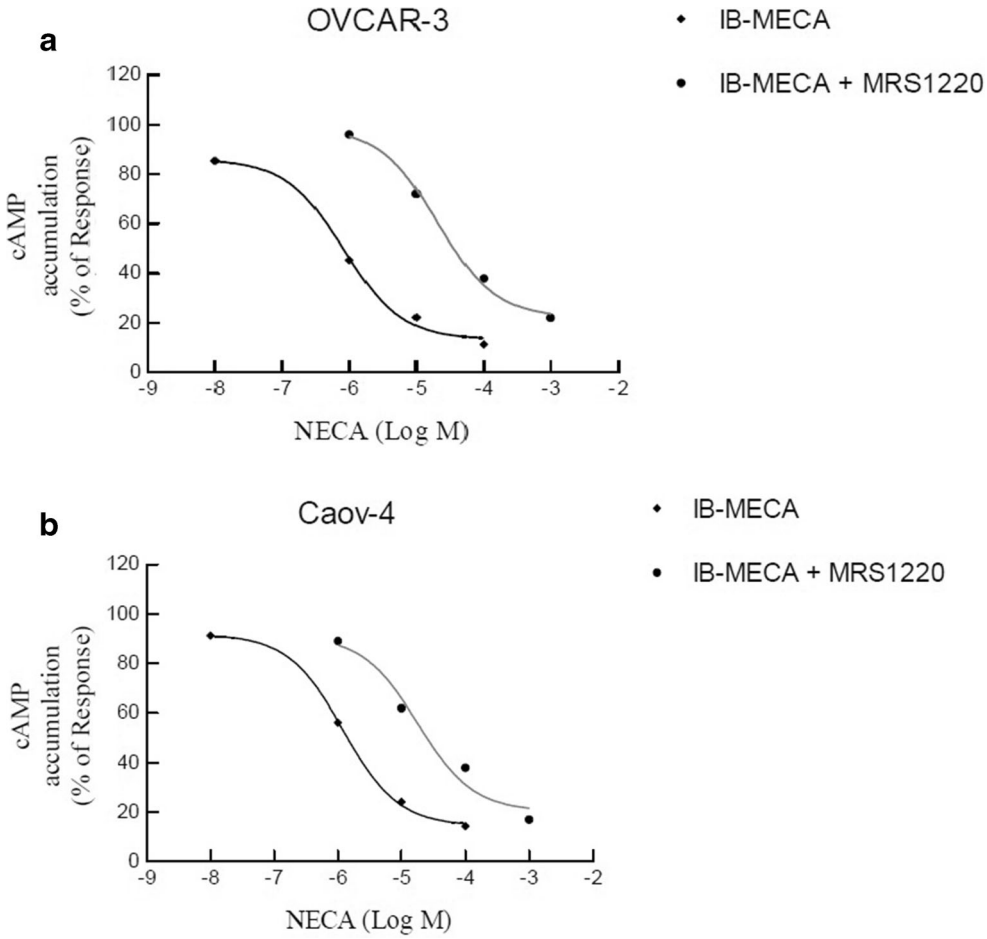

Fig. 2 Effect of A_3 adenosine receptor agonist and antagonist on cyclic AMP accumulation. OVCAR-3 (**a**) and Caov-4 (**b**) cells were treated with increasing concentrations of IB-MECA in the presence and absence of MRS1220 (1 μM), and then cAMP accumulation was carried out using colorimetric competitive ELISA kit. Data are given as percentage. Each point is the mean±SD of three experiments. Each experiment was repeated three times

Antiproliferative effect of IB-MECA in human ovarian cancer cell lines

To evaluate the effects of IB-MECA on the viability of OVCAR-3 and Caov-4 ovarian cancer cells, the MTT assay was carried out. The MTT assay measures the activity of mitochondrial dehydrogenase enzyme based on its ability of cleaving tetrazolium ring to produce formazan; thus, the assay can be used as an index of cell viability. Treatment of cell lines with the IB-MECA for 48 h resulted in a dose-dependent reduction in the cell viability when compared with that of the control (Fig. 3). In the OVCAR-3 cells, as indicated in Fig. 3a, a significant inhibitory effect was observed at 0.1 μM ($P<0.05$ versus the control group) which reached maximum at 100 μM ($P<0.01$ versus the control group). Similarly, in the Caov-4 cells (Fig. 3b), a significant decrease has been observed in the cell viability at 0.1–100 μM ($P<0.01$). The IC_{50}s (the effective dose that inhibits 50 % growth) for treatment of OVCAR-3 and Caov-4 cells by IB-MECA were 32.14 and 45.37 μM, respectively. To demonstrate the specificity of A_3 adenosine receptors in the inhibition of cell viability, both cell lines were pretreated with the A_3 adenosine receptor antagonist, MRS1220 (1 μM). As shown in Fig. 3, the inhibitory effects of IB-MECA on cell growth were significantly blocked by MRS1220 (1 μM) in both cell lines. It is important to note that MRS1220 has no effects on cell growth when used alone in different concentrations (0.0001–10 μM) (data not shown).

Detection of apoptosis by flow cytometry

To investigate whether the IB-MECA-induced cell growth inhibition was related to apoptosis, the effect of IB-MECA on cell apoptosis was evaluated. Both cell lines were incubated at various concentrations (0.1–100 μM) of IB-MECA for 48 h and analyzed by flow cytometry using annexin V and PI double staining. A significant increase in the percentage of apoptosis in a concentration-dependent manner is shown ($P<0.05$). As shown in Fig. 4a, apoptosis ranged from 4±0.5 to 39.1±4.6 % in OVCAR-3 cell line. Caov-4-treated cells indicated that apoptosis ranged from 3.7±0.8 to 36.8±5.1 % (Fig. 4c). Further confirmation of the involvement of A_3 adenosine receptor in the induction of apoptosis by IB-MECA was provided by the results obtained from pretreatment of the

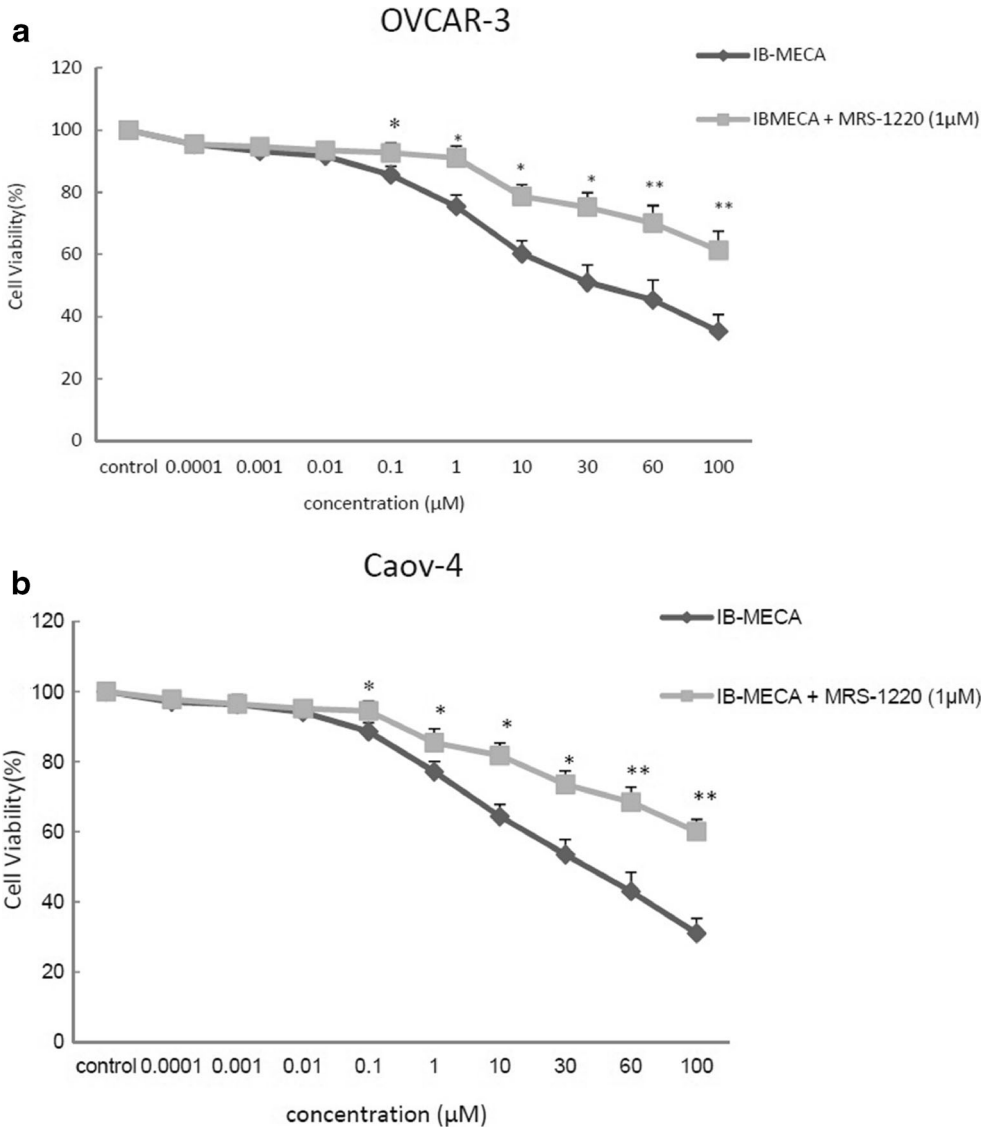

Fig. 3 The effect of IB-MECA on cell viability was measured using the MTT assay. OVCAR-3 (**a**) and Caov-4 (**b**) cells were treated with different concentrations of IB-MECA in the presence and absence of MRS1220 (A_3AR antagonist) and incubated for 48 h. The MTT assay was carried out as described in the "Materials and methods." Each value is presented as mean±SD of three experiments. Each experiment was conducted in triplicate. *$P<0.05$; **$P<0.01$ compared with the untreated control group

cells with MRS1220, as an A_3AR antagonist. MRS1220 inhibited IB-MECA-induced apoptosis in the cell lines (Fig. 4a, c).

In order to confirm that IB-MECA induces apoptosis in OVCAR-3 and Caov-4 cells, the anti-apoptotic protein, Bcl-2, and the pro-apoptotic protein, Bax, were evaluated. The results of western blot analysis showed that the expression of Bcl-2 was noticeably decreased in response to the treatment with IB-MECA, while the expression of Bax protein was steadily increased (Fig. 5a, b). These findings suggest that the Bcl-2 family of proteins is involved in the apoptosis induced by IB-MECA.

Involvement of caspases in IB-MECA-induced apoptosis

To explore the possible biochemical mechanisms underlying IB-MECA-induced apoptosis, the activation of caspases-3 and caspase-9 was investigated. The findings showed that treatment of both cells with various concentrations of IB-MECA induced a significant increase in the activity of caspase-3 and caspase-9 in a dose-dependent manner (Fig. 6) ($P<0.05$). Furthermore, the results demonstrated that treatment of cells with IB-MECA (10 μM) resulted in a significant increase ($P<0.05$) of caspase-3 and caspase-9, in a time-dependent manner (Fig. 6c). To further confirm the involvement of caspases in the induction of apoptosis by IB-MECA, cells were pretreated with Z-VAD-fmk, as a broad spectrum caspase inhibitor. The effects of Z-VAD-FMK on the inhibition of apoptosis were measured after incubation with different concentrations of IB-MECA. This caspase inhibitor prevented apoptosis, as measured by annexin V and PI (Fig. 7). Thus, it appears that in the ovarian cancer cell line, apoptosis was induced by IB-MECA through the caspase pathway.

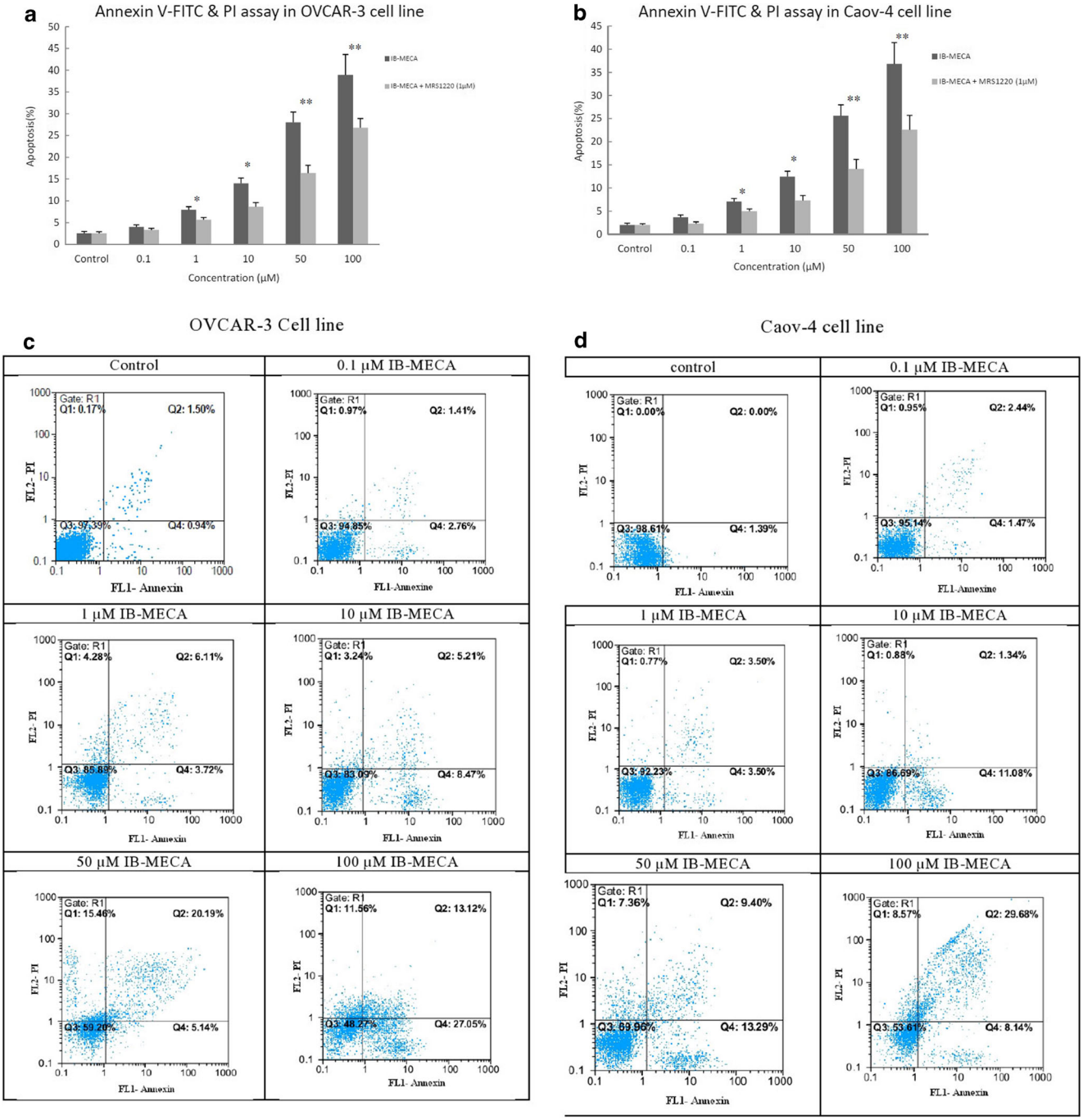

Fig. 4 Detection of apoptosis using flow cytometry. Flow cytometric analysis of OVCAR-3 (**a**) and Caov-4 (**c**) after treatment with various concentrations of IB-MECA in the presence and absence of MRS1220 (A_3AR antagonist) for 48 h. FACS histograms of annexin V-FITC/PI staining that were analyzed using the software supplied in the instrument (**b**, **d**). The results shown represent the mean±SD of three independent experiments. *P<0.05; **P<0.01 compared with the control group

Role of mitochondrial membrane potential in IB-MECA-induced cell apoptosis

Another biochemical marker of the apoptotic process is loss of mitochondria membrane potential (ΔΨm). Therefore, ΔΨm was measured after treatment of OVCAR-3 and Caov-4 cells with different concentrations of IB-MECA (0.1–100 μM). JC-1, a cationic dye which exhibits potential-dependent accumulation in the mitochondria, was employed to determine the loss in ΔΨm. The results showed that a significant loss of ΔΨm occurred after treatment with IB-MECA and the depletion of mitochondrial membrane potential (MMP) increased in a dose-dependent manner (Fig. 8). In order to confirm the involvement of MMP in the induction of apoptosis by IB-

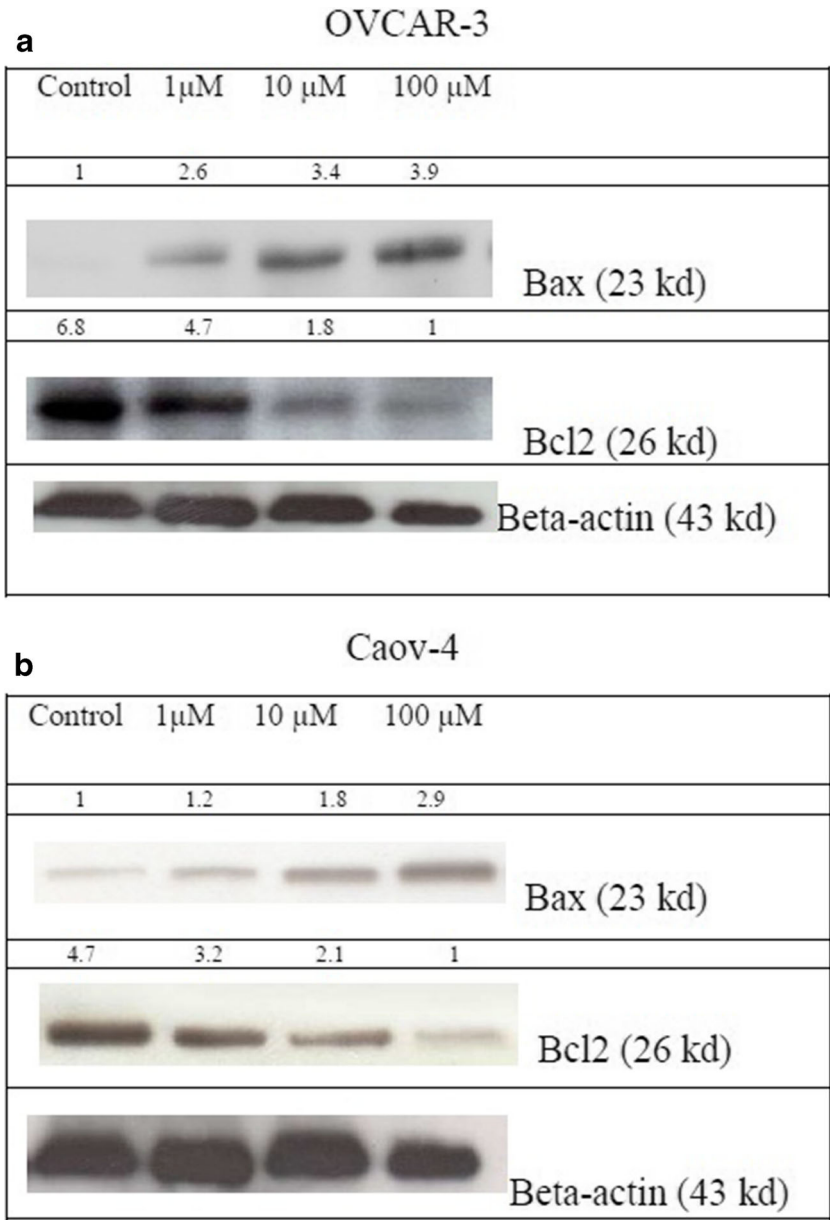

Fig. 5 The effects of IB-MECA on the expression of Bcl-2 and Bax apoptosis-related proteins. OVCAR-3 (**a**) and Caov-4 (**b**) cells were treated with different concentrations of IB-MECA for 48 h. Total cellular proteins were prepared and the expressions of Bcl-2 and Bax proteins were analyzed using western blotting. The expression of Bcl-2 was noticeably decreased in response to the treatment with IB-MECA, while the expression of Bax protein was steadily increased. Beta-actin was used as an internal control

MECA, cells were pretreated with the A_3AR antagonist, MRS1220. The results showed that loss of $\Delta\Psi m$ by IB-MECA was suppressed significantly ($P<0.05$) in both cell lines (Fig. 8). Furthermore, the results demonstrated that treatment of cells with IB-MECA (10 μM) resulted in a significant decrease ($P<0.05$) of MMP, in a time-dependent manner (Fig. 8c).

Discussion

Numerous studies have revealed that adenosine exerts its antiproliferative effect mainly through activation of A_3AR [29–31]. The A_3AR agonists play a key role in the inhibition of tumor growth, both in vitro and in vivo [18, 32]. Previous studies demonstrated that A_3AR mediates apoptosis in human cancer cell lines such as breast, lung, bladder, prostate, hepatocellular carcinoma, leukemia, and thyroid [22, 24, 25, 33–36]. In addition, safety and good tolerance of the A_3AR agonists in humans were indicated in preclinical and phase I studies [37]. Therefore, A_3AR agonists especially IB-MECA and CL-IB-MECA have been considered as potential antitumor and possible therapeutic agents to various cancers.

It was reported that IB-MECA can inhibit proliferation of prostate cancer cell lines DU-145, PC3, and LNcap via arresting cell cycle progression and induction of apoptosis [22]. A_3AR agonists also exhibited antiproliferative effects in both estrogen receptor-positive and receptor-negative breast cancer

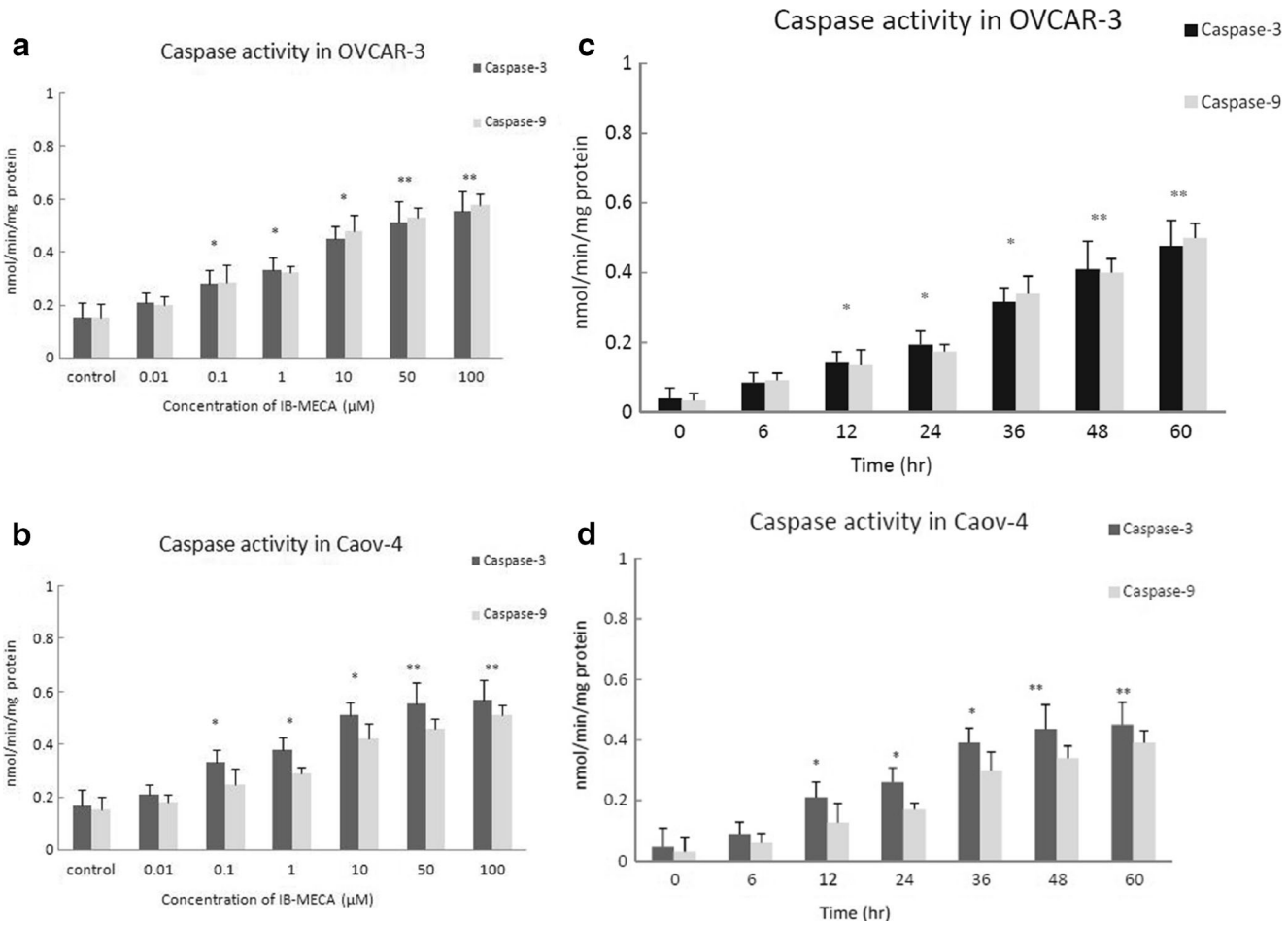

Fig. 6 Colorimetric assay of caspase-3 and caspase-9 activities after treatment with IB-MECA for 48 h. In OVCAR-3 cells (**a**), the activity of caspase-3 and caspase-9 increased in a concentration-dependent manner. The activity of caspase-3 and caspase-9 increased in a concentration-dependent manner in Caov-4 cells (**b**). To examine the effect of time-dependent caspase-3 and caspase-9 activity, cells were treated with 10 μM concentration of IB-MECA and incubated in a time interval between 0 and 60 h (**c**, **d**). *$P<0.05$; **$P<0.01$ compared with the control group

cells [23]. Recently, the effects of adenosine on ovarian cancer cells have been investigated. An increase in sub-G1 population, activation of caspase-3, downregulation of Bcl-2 protein, and upregulation of Bax protein expression level were observed after treatment with adenosine. These results showed that adenosine can inhibit ovarian cancer cell proliferation through G1 cell cycle arrest and induction of apoptosis [7]. But the effects of IB-MECA and other A_3AR agonists in human ovarian cancer cell lines have not been investigated. In the present study, mRNA and protein expression of A_3 adenosine receptor have been shown in both cell lines at different levels. To verify whether the increase in A_3 receptor expression was reflected in the regulation of second messengers activated by A_3 adenosine receptor, the ability of A_3 agonist and antagonist in modulating adenylyl cyclase activity was investigated. Both cell lines had a decrease level in cyclic AMP after exposure with different concentrations of IB-MECA, whereas MRS1220 (the antagonist of A_3) reversed the agonist effect. Moreover, our results indicated that the mRNA expression of A_3 in Caov-4 cells was higher than OVCAR-3 cells, but there are no significant differences in protein expression and cAMP accumulation, which could be due to the degradation of A_3 adenosine receptor mRNA or protein. These results demonstrate that, despite the difference in the amount of mRNA expression, the function of both cells in response to IB-MECA is almost identical.

In some previous studies, the expression levels of adenosine receptor subtypes were explored, and different levels of expression in each subtype were reported. Aghaei et al. demonstrated that mRNAs of A_3 adenosine receptor have the most expression compared with other receptors in prostate cancer cell lines. Moreover, they showed that IB-MECA dose-dependently reduces the accumulation of cyclic AMP in prostate cancer cell lines, thus suggesting a functional role of the A_3 adenosine receptor [22]. Other investigations reported that cAMP levels were decreased in response to IB-MECA in MCF-7 breast cancer cell line [38]. One adenosine receptor

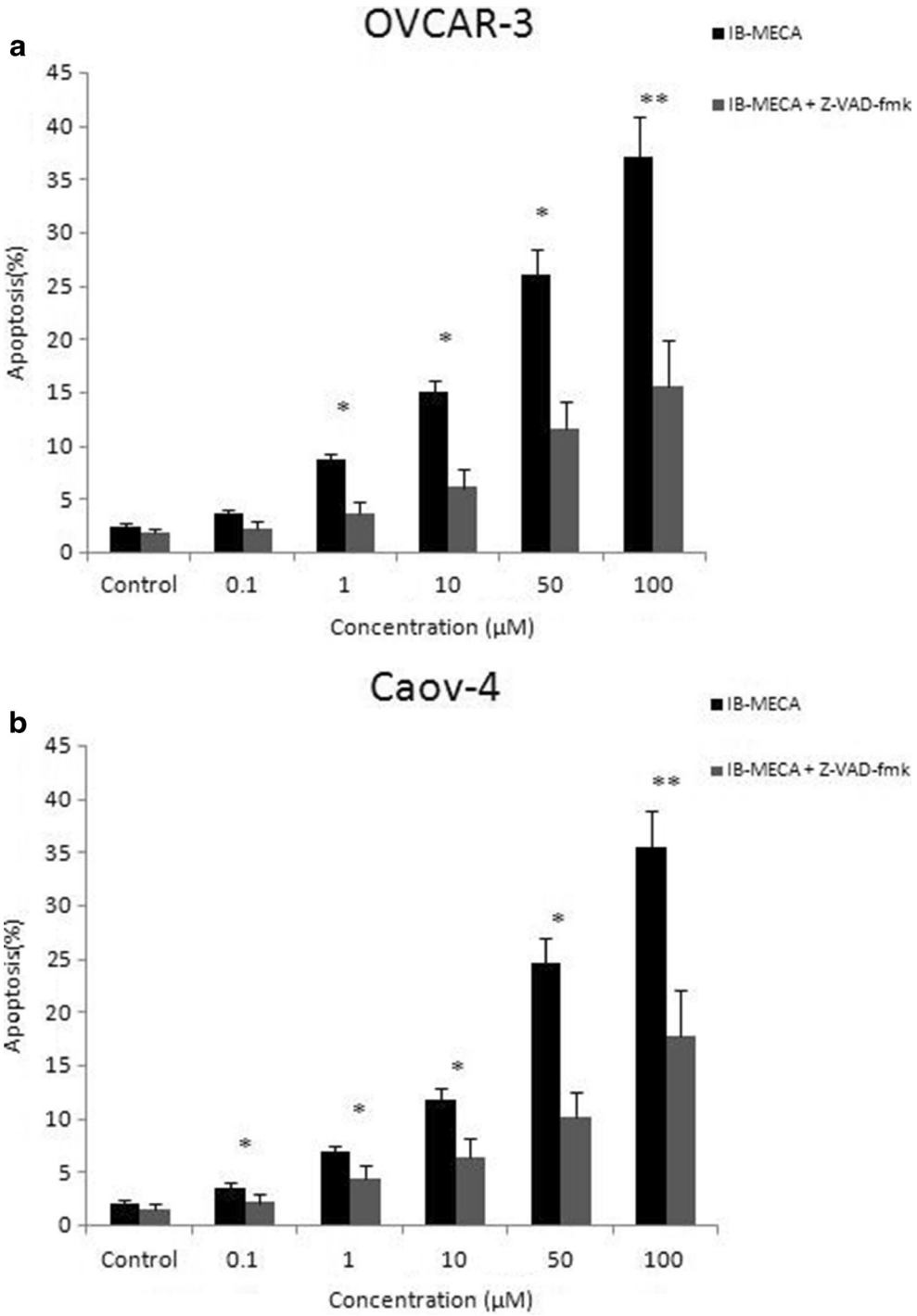

Fig. 7 The effects of caspase inhibition on IB-MECA-induced apoptosis in OVCAR-3 (**a**) and Caov-4 (**b**) ovarian cancer cells. Cells were pretreated with Z-VAD-fmk and then were treated with various concentrations of IB-MECA for 48 h. Z-VAD-fmk significantly inhibited IB-MECA-induced apoptosis in both cells. *$P<0.05$ and **$P<0.01$ are significant. Statistical analysis was performed by ANOVA. *Each point* represents three repeats of triplicate

may also be coupled to more than one G protein. This is common after transfection. After activation of the G proteins, enzymes and ion channels are affected as can be predicted from what is known about G protein signaling. Thus, A_3 adenosine receptors mediate inhibition of adenylyl cyclase, activation of phospholipase C, etc. In CHO cells transfected with the human A_3 adenosine receptor, both adenylyl cyclase inhibition and a Ca^{2+} signal are mediated via a Gi/o-dependent pathway [11].

We examined the growth inhibitory effect of IB-MECA in the presence and absence of A_3 antagonist (MRS1220) on two human ovarian cancer cell lines and possible mechanism of action. In the present study, A_3AR agonist (IB-MECA) exerted a dose-dependent inhibitory effect on OVCAR-3 and Caov-4 ovarian cancer cells (Fig. 3). The antagonist of A_3 adenosine receptor inhibited the agonist effect of IB-MECA in both cell lines (Fig. 3).

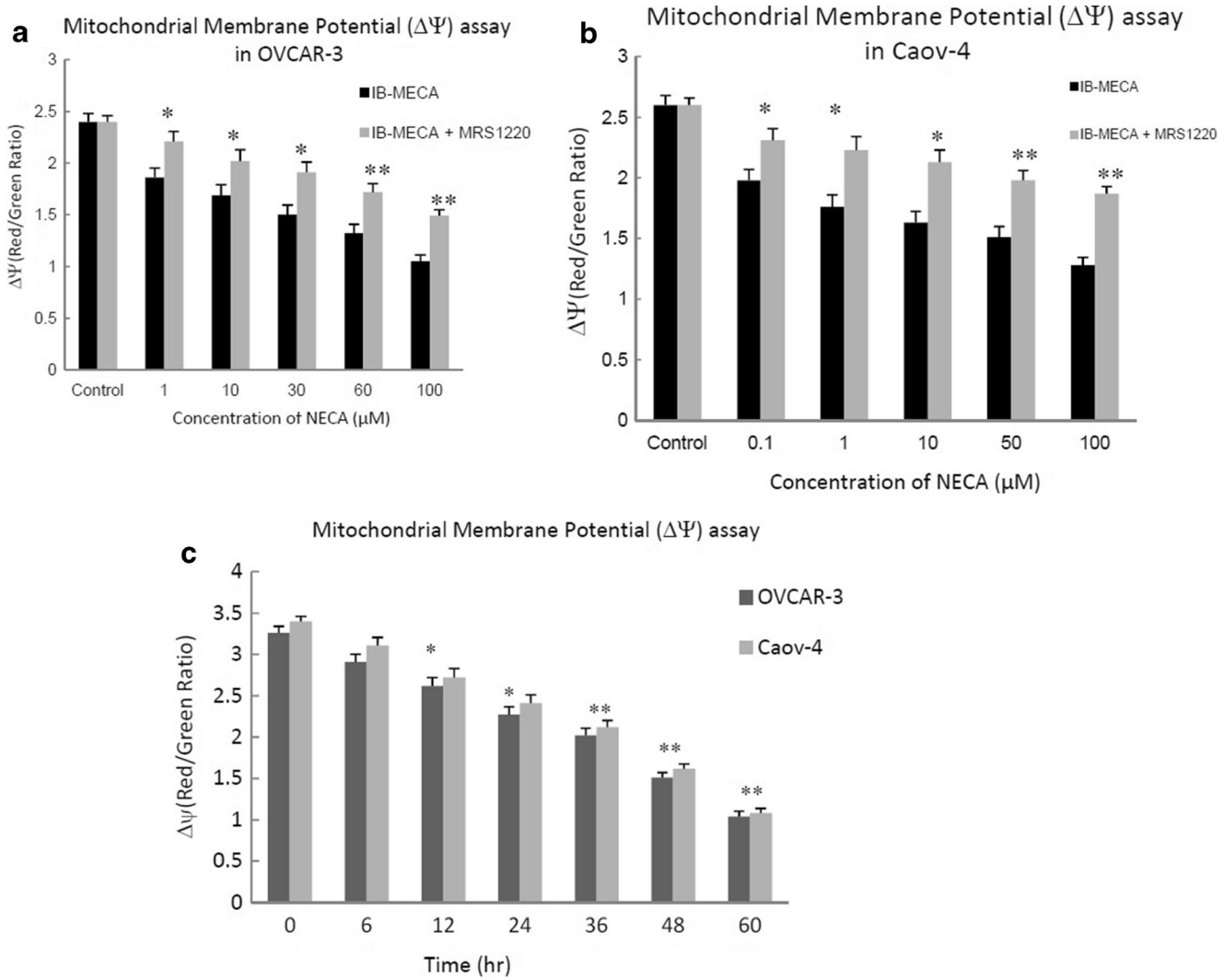

Fig. 8 Detection of mitochondrial membrane potential (MMP) in IB-MECA-induced cell apoptosis. After treatment, cells with different concentrations of IB-MECA for 48 h with and without of A_3AR antagonist, MRS1220, were loaded with JC-1 dye and the potential-dependent accumulation in the mitochondria (reduced $\Delta\Psi m$ indicated by a decrease in red/green fluorescence) measured directly in OVCAR-3 (**a**) and Caov-4 (**b**) cell lines. To examine the effect of time in depletion of MMP, cells were treated with 10 μM concentration of IB-MECA and incubated in a time interval between 0 and 60 h (**c**). The data represent the average values from triplicates of three independent experiments. *$P<0.05$ is significant. Statistical analysis was performed by ANOVA

Our results demonstrated that IB-MECA inhibited the proliferation of human ovarian cancer cells through inducing apoptosis. These findings are similar to the results in lung cancer [34], breast cancer [23], and prostate cancer cell lines [22] treated with A_3AR agonists. Apoptosis is characterized by a variety of biochemical features that are used to discriminate apoptotic cell death.

Caspases, a family of cysteine proteases, play an integral role in apoptotic cell death [39]. For the major pathway for caspase activation, mitochondrial damage releases cytochrome c that forms an oligomeric complex with dATP or apoptosis proteases activating factor-1 (Apf-1), and the complex activates caspase-9 and the effector caspases, caspase-3 [39]. Kim et al. demonstrated that A_3AR agonist induced cell death through activating caspase-mediated apoptotic process in human lung cancer cells, which was manifested by activation of caspase-3 and caspase-9 [33]. Furthermore, involvement of caspase-3 in the apoptotic effect of adenosine in human colon cancer cells was reported previously [40, 41]. Shieh et al. investigated the role of caspase-3 in the induction of apoptosis in HepG2/C3A cells. They found that the activity of caspase-3 reached to a maximal value 48 h after treatment [42]. Moreover, Shirali et al. reported that treatment of ovarian cancer cells with adenosine increases the activity of caspase-3, and the caspase-3 inhibitor is capable of protecting cells from the cytotoxic effect of adenosine. Thus, it appeared that apoptosis was induced by adenosine through the caspase pathway in ovarian cancer cells [7]. In the present study, IB-MECA

activated caspase-9 and the effector caspase, caspase-3, in both cell lines. This implies that IB-MECA is engaged in the activation of caspase-9 and the ensuing caspase-3. Moreover, we demonstrated that caspase-3 inhibition is capable of protecting cells from apoptotic effect of IB-MECA. Peptidyl-fluoromethylketones such as Z-VAD-fmk (benzyloxycarbonyl-Val-Ala-Asp-fluoromethyl-ketone) are irreversible inhibitors of cysteine proteases. Z-VAD-fmk was designed to enter live cells as the O-methyl ester (of the aspartyl carboxy side chain) and to be converted by intracellular esterases into the active inhibitor [43]. Cells were treated with various concentrations of IB-MECA in the presence of Z-VAD-fmk. Z-VAD-fmk co-treatment abolished the apoptotic effects of IB-MECA-treated cell lines (Fig. 7). Z-VAD-fmk alone did not affect the cells. This finding also suggests a role for caspase in the IB-MECA-induced cell apoptosis.

Apoptosis is controlled by pro-apoptotic and anti-apoptotic proteins. The cellular Bcl-2 has been shown to delay or block apoptosis induced by numerous physiological and pathological stimuli. Bcl-2 heterodimerizes with a conserved homologue, Bax, that accelerates programmed cell death [44]. We found that IB-MECA decreased the expression of Bcl-2 in OVCAR-3 and Caov-4 cell lines, whereas the expression of Bax increased. These results suggest that activation of A_3 receptor evokes signals that are involved in the regulation of Bcl-2 and Bax proteins. There have been a number of studies showing changes in endogenous levels of Bcl-2 in response to apoptotic stimuli. For example, both p53 and transforming growth factor-α1 (TGF-α1) decreased Bcl-2 expression [45]. Overexpression of Bcl-2 protected OVCAR-3 and Caov-4 cells from IB-MECA-induced apoptosis, suggesting that the inhibitory effect of IB-MECA on endogenous Bcl-2 expression is involved in the apoptotic effect of this agonist on OVCAR-3 and Caov-4 cells. The incomplete protection by the exogenous Bcl-2 can be due to the induction of pro-apoptotic proteins or the activation of caspases, which cleave Bcl-2 by IB-MECA. Indeed, we found that IB-MECA induced activation of caspase-3 in OVCAR-3 and Caov-4 cells and that inhibition of caspase-3 (using caspase-3 inhibitor, Z-VAD-fmk) abolished the apoptosis induced by IB-MECA.

The role of MMP in the apoptosis induced by adenosine receptors was investigated in several cancer cell lines [46–48]. It was demonstrated that adenosine induced apoptosis via loss of MMP in EL-4 thymoma cells [46]. The present results have also shown that IB-MECA increased the loss of MMP ($\Delta\Psi m$) in both cell lines in a concentration-dependent manner (Fig. 8). The levels of MMP ($\Delta\Psi m$) loss were similar to those of annexin V staining cells, implying that induction of cell apoptosis by IB-MECA was tightly correlated with the collapse of MMP ($\Delta\Psi m$).

Conclusion

The present study showed a possible mechanism for the control of ovarian cancer cell growth through A_3 adenosine receptor activation. The results illustrated that IB-MECA inhibits OVCAR-3 and Caov-4 ovarian cancer cell proliferation via induction of apoptosis. Apoptosis induced by IB-MECA was also determined by loss of MMP, activation of caspase-3 and caspase-9, and downregulation of Bcl-2 protein expression, which indicated that the mitochondrial pathway was also involved in the apoptotic signaling pathway.

Acknowledgments This work was supported by grants from Isfahan University of Medical Sciences.

Conflicts of interest None

References

1. Parmar M, Ledermann J, Colombo N, Du Bois A, Delaloye J, Kristensen G, et al. Paclitaxel plus platinum-based chemotherapy versus conventional platinum-based chemotherapy in women with relapsed ovarian cancer: the ICON4/AGO-OVAR-2.2 trial. Lancet. 2003;361:2099–106.
2. Stewart DE, Wong F, Cheung A, Dancey J, Meana M, Cameron J, et al. Information needs and decisional preferences among women with ovarian cancer. Gynecol Oncol. 2000;77:357–61.
3. Siegel R, Ma J, Zou Z, Jemal A. Cancer statistics, 2014. CA Cancer J Clin. 2014;64:9–29.
4. Thompson CB. Apoptosis in the pathogenesis and treatment of disease. Science. 1995;267:1456–62.
5. Kamesaki H. Mechanisms involved in chemotherapy-induced apoptosis and their implications in cancer chemotherapy. Int J Hematol. 1998;68:29–43.
6. Janssens R, Boeynaems JM. Effects of extracellular nucleotides and nucleosides on prostate carcinoma cells. Br J Pharmacol. 2001;132:536–46.
7. Shirali S, Aghaei M, Shabani M, Fathi M, Sohrabi M, Moeinifard M. Adenosine induces cell cycle arrest and apoptosis via cyclinD1/Cdk4 and Bcl-2/Bax pathways in human ovarian cancer cell line OVCAR-3. Tumor Biol. 2013;34(2):1085–95.
8. St Hilaire C, Carroll SH, Chen H, Ravid K. Mechanisms of induction of adenosine receptor genes and its functional significance. J Cell Physiol. 2009;218:35–44.
9. Gessi S, Merighi S, Sacchetto V, Simioni C, Borea PA. Adenosine receptors and cancer. Biochim Biophys Acta. 2011;1808:1400–12.
10. Fredholm BB, IJzerman AP, Jacobson KA, Klotz K-N, Linden J. International Union of Pharmacology. XXV. Nomenclature and classification of adenosine receptors. Pharmacol Rev. 2001;53:527–52.
11. Poulsen SA, Quinn RJ. Adenosine receptors: new opportunities for future drugs. Bioorg Med Chem. 1998;6:619–41.
12. Abbracchio MP. P1 and P2 receptors in cell growth and differentiation. Drug Dev Res. 1996;39:393–406.
13. Madi L, Ochaion A, Rath-Wolfson L, Bar-Yehuda S, Erlanger A, Ohana G, et al. The A3 adenosine receptor is highly expressed in tumor versus normal cells potential target for tumor growth inhibition. Clin Cancer Res. 2004;10:4472–9.
14. Brambilla R, Cattabeni F, Ceruti S, Barbieri D, Franceschi C, Kim Y-C, et al. Activation of the A3 adenosine receptor affects cell cycle

progression and cell growth. Naunyn Schmiedeberg's Arch Pharmacol. 2000;361:225–34.
15. Tanaka Y, Yoshihara K, Tsuyuki M, Kamiya T. Apoptosis induced by adenosine in human leukemia HL-60 cells. Exp Cell Res. 1994;213: 242–52.
16. Fishman P, Madi L, Bar-Yehuda S, Barer F, Del Valle L, Khalili K. Evidence for involvement of Wnt signaling pathway in IB-MECA mediated suppression of melanoma cells. Oncogene. 2002;21:4060–4.
17. Abbracchio MP, Ceruti S, Brambilla R, Franceschi C, Malorni W, Jacobson KA, et al. Modulation of apoptosis by adenosine in the central nervous system: a possible role for the A3 receptor. Ann N Y Acad Sci. 1997;825:11–22.
18. Fishman P, Bar-Yehuda S, Ohana G, Barer F, Ochaion A, Erlanger A, et al. An agonist to the A3 adenosine receptor inhibits colon carcinoma growth in mice via modulation of GSK-3β and NF-κB. Oncogene. 2004;23:2465–71.
19. Kohno Y, Sei Y, Koshiba M, Kim HO, Jacobson KA. Induction of apoptosis in HL-60 human promyelocytic leukemia cells by adenosine A(3) receptor agonists. Biochem Biophys Res Commun. 1996;219:904–10.
20. Lu J, Pierron A, Ravid K. An adenosine analogue, IB-MECA, down-regulates estrogen receptor α and suppresses human breast cancer cell proliferation. Cancer Res. 2003;63:6413–23.
21. Madi L, Bar-Yehuda S, Barer F, Ardon E, Ochaion A, Fishman P. A3 adenosine receptor activation in melanoma cells: association between receptor fate and tumor growth inhibition. J Biol Chem. 2003;278: 42121–30.
22. Aghaei M, Panjehpour M, Karami-Tehrani F, Salami S. Molecular mechanisms of A3 adenosine receptor-induced G1 cell cycle arrest and apoptosis in androgen-dependent and independent prostate cancer cell lines: involvement of intrinsic pathway. J Cancer Res Clin Oncol. 2011;137:1511–23.
23. Panjehpour M, Karami-Tehrani F. An adenosine analog (IB-MECA) inhibits anchorage-dependent cell growth of various human breast cancer cell lines. Int J Biochem Cell Biol. 2004;36:1502–9.
24. Panjehpour M, Karami-Tehrani F. Adenosine modulates cell growth in the human breast cancer cells via adenosine receptors. Oncol Res. 2007;16:575–85.
25. Bar-Yehuda S, Stemmer S, Madi L, Castel D, Ochaion A, Cohen S, et al. The A3 adenosine receptor agonist CF102 induces apoptosis of hepatocellular carcinoma via de-regulation of the Wnt and NF-κB signal transduction pathways. Int J Oncol. 2008;33:287.
26. Hashemi M, Karami-Tehrani F, Ghavami S, Maddika S, Los M. Adenosine and deoxyadenosine induces apoptosis in oestrogen receptor-positive and -negative human breast cancer cells via the intrinsic pathway. Cell Prolif. 2005;38:269–85.
27. Ghavami S, Eshragi M, Ande SR, Chazin WJ, Klonisch T, Halayko AJ, et al. S100A8/A9 induces autophagy and apoptosis via ROS-mediated cross-talk between mitochondria and lysosomes that involves BNIP3. Cell Res. 2010;20:314–31.
28. Ghavami S, Kerkhoff C, Chazin WJ, Kadkhoda K, Xiao W, Zuse A, et al. S100A8/9 induces cell death via a novel, RAGE-independent pathway that involves selective release of Smac/DIABLO and Omi/HtrA2. Biochim Biophys Acta. 2008;1783:297–311.
29. Ohana G, Bar-Yehuda S, Barer F, Fishman P. Differential effect of adenosine on tumor and normal cell growth: focus on the A3 adenosine receptor. J Cell Physiol. 2001;186:19–23.
30. Merighi S, Mirandola P, Milani D, Varani K, Gessi S, Klotz K-N, et al. Adenosine receptors as mediators of both cell proliferation and cell death of cultured human melanoma cells. J Investig Dermatol. 2002;119:923–33.
31. Fishman P, Bar-Yehuda S, Madi L, Cohn I. A3 adenosine receptor as a target for cancer therapy. Anti Cancer Drug. 2002;13:437–43.
32. Fishman P, Bar-Yehuda S, Ardon E, Rath-Wolfson L, Barrer F, Ochaion A, et al. Targeting the A3 adenosine receptor for cancer therapy: inhibition of prostate carcinoma cell growth by A3AR agonist. Anticancer Res. 2003;23:2077–84.
33. Kim S-J, Min H-Y, Chung H-J, Park E-J, Hong J-Y, Kang Y-J, et al. Inhibition of cell proliferation through cell cycle arrest and apoptosis by thio-Cl-IB-MECA, a novel A3 adenosine receptor agonist, in human lung cancer cells. Cancer Lett. 2008;264:309–15.
34. Kim H, Kang JW, Lee S, Choi WJ, Jeong LS, Yang Y, et al. A3 adenosine receptor antagonist, truncated Thio-Cl-IB-MECA, induces apoptosis in T24 human bladder cancer cells. Anticancer Res. 2010;30:2823–30.
35. Mlejnek P, Dolezel P. Induction of apoptosis by A3 adenosine receptor agonist N6-(3-iodobenzyl)-adenosine-5′-N-methylcarboxamide in human leukaemia cells: a possible involvement of intracellular mechanism. Acta Physiol. 2010;199:171–9.
36. Morello S, Sorrentino R, Porta A, Forte G, Popolo A, Petrella A, et al. Cl-IB-MECA enhances TRAIL-induced apoptosis via the modulation of NF-κB signalling pathway in thyroid cancer cells. J Cell Physiol. 2009;221:378–86.
37. Fishman P, Bar-Yehuda S, Synowitz M, Powell J, Klotz K, Gessi S, et al. Adenosine receptors and cancer. Handb Exp Pharmacol. 2009;193:399–441.
38. Panjehpour M, Castro M, Klotz KN. Human breast cancer cell line MDA-MB-231 expresses endogenous A2B adenosine receptors mediating a Ca2+ signal. Br J Pharmacol. 2005;145:211–8.
39. Alnemri ES, Livingston DJ, Nicholson DW, Salvesen G, Thornberry NA, Wong WW, et al. Human ICE/CED-3 protease nomenclature. Cell. 1996;87:171.
40. Saito M, Yaguchi T, Yasuda Y, Nakano T, Nishizaki T. Adenosine suppresses CW2 human colonic cancer growth by inducing apoptosis via A(1) adenosine receptors. Cancer Lett. 2010;290:211–5.
41. Yasuda Y, Saito M, Yamamura T, Yaguchi T, Nishizaki T. Extracellular adenosine induces apoptosis in Caco-2 human colonic cancer cells by activating caspase-9/-3 via A2a adenosine receptors. J Gastroenterol. 2009;44:56–65.
42. Shieh D-E, Chen Y-Y, Yen M-H, Chiang L-C, Lin C-C. Emodin-induced apoptosis through p53-dependent pathway in human hepatoma cells. Life Sci. 2004;74:2279–90.
43. Dolle RE, Hoyer D, Prasad CV, Schmidt SJ, Helaszek CT, Miller RE, et al. P1 aspartate-based peptide alpha-((2,6-dichlorobenzoyl)oxy)methyl ketones as potent time-dependent inhibitors of interleukin-1 beta-converting enzyme. J Med Chem. 1994;37:563–4.
44. Korsmeyer SJ. BCL-2 gene family and the regulation of programmed cell death. Cancer Res. 1999;59:1693s–700s.
45. Miyashita T, Krajewski S, Krajewska M, Wang HG, Lin HK, Liebermann DA, et al. Tumor suppressor p53 is a regulator of bcl-2 and bax gene expression in vitro and in vivo. Oncogene. 1994;9: 1799–805.
46. El-Darahali A, Fawcett H, Mader JS, Conrad DM, Hoskin DW. Adenosine-induced apoptosis in EL-4 thymoma cells is caspase-independent and mediated through a non-classical adenosine receptor. Exp Mol Pathol. 2005;79:249–58.
47. Sai K, Yang D, Yamamoto H, Fujikawa H, Yamamoto S, Nagata T, et al. A(1) adenosine receptor signal and AMPK involving caspase-9/-3 activation are responsible for adenosine-induced RCR-1 astrocytoma cell death. Neurotoxicology. 2006;27:458–67.
48. Wu LF, Li GP, Feng JL, Pu ZJ. Molecular mechanisms of adenosine-induced apoptosis in human HepG2 cells. Acta Pharmacol Sin. 2006;27:477–84.